Volume 1, Number 1, 2008. pp. 1-8

Jordan Journal of Physics

ARTICLE

Time-Dependent Response of Field Emission by Single Carbon Nanotubes

M. J. Hagmann[a] and **M. S. Mousa**[b]

[a] *New Path Research, Salt Lake City, Utah 84110, USA.*
[b] *Department of Physics, Mu'tah University, Al-Karak, Jordan.*

Received on: 9/5/2007; Accepted on: 8/5/2008

Abstract: Four field emission tubes that have single carbon nanotubes (CNT) as the emitters were tested; two with single-walled CNT and two with multiwalled CNT. A tube with a tungsten tip was used for comparison. Fowler-Nordheim analysis of the DC current-voltage data gave reasonable values for the local fields at the emitters and the sizes of the emitters. Two oscillators were used to superimpose sinusoidal signals on the applied static field, thus increasing the DC emitted current and causing a mixer current at their difference frequency, in agreement with theory. Square-wave pulses from a single laser diode (20 mW, 658 nm) focused on each emitter increased the emitted current by 5.2% with the CNT and 0.19% with the tungsten tip.
Keywords: Field Emission, Carbon Nanotubes, Fowler-Nordheim analysis.

Introduction

Simulations and preliminary experiments show that photomixing (optical heterodyning) in laser-assisted field emission could be used as a new microwave or terahertz (THz) source, with a multi-octave bandwidth [1]. The field emitter tip is much smaller than the wavelength of the incident optical radiation so quasi-static conditions require that the electric field of the radiation is superimposed on the applied static field to modulate the height of the barrier. Electrons tunnel from the tip into vacuum with a delay τ of less than 2 fs [2]. Thus, because the current-voltage characteristics of field emission are extremely nonlinear, if two lasers are focused on the tip, the mixer current would follow each cycle of the difference frequency of the two lasers from DC up to 500 THz ($1/\tau$). The tip will withstand applied static fields as high as 9 V/nm [3], so that incident laser radiation with comparable field strengths could produce a bright source of microwave or THz radiation.

Carbon nanotubes (CNT) are excellent field emitters and facilitate the miniaturization of electron devices [4]. Furthermore, the kinetic inductance of CNT causes them to be high impedance (~5 kΩ) transmission lines [5, 6], and we have shown that this effect can be used for efficient broadband matching to the high impedance that is inherent in field emission [7]. We will describe the static and dynamic characterization of field emitters consisting of single CNT, both single-walled (SWCNT) and multiwalled (MWCNT), and compare them to a field emitter consisting of an etched single crystal of tungsten. We acknowledge that some of this information was first presented in a paper at an international conference [8].

Description and Static Characterization of the Field Emitters

Four field emission tubes, as shown in Fig. 1, were made for us by Xintek (Chapel Hill, NC). The copper anode is at the right, and the CNT emitter is mounted on a tungsten wire attached to the copper cylinder at the left. Fig. 2 shows images of the CNT emitters for each tube, taken with a

Corresponding Author: M. J. Hagmann. **Email**: MHagmann@NewPathResearch.Com.

JEOL model JEM 6300 SEM. Tubes M-1 and M-4 have a single MWCNT as the emitter, and tubes C-3 and C-6 have a single SWCNT as the emitter. The CNT are in bundles that have diameters of 10 to 30 nm, but in each tube the field emission is from the one CNT at the end of the bundle where the electric field is most intense. The dimensions of the individual CNT were not determined.

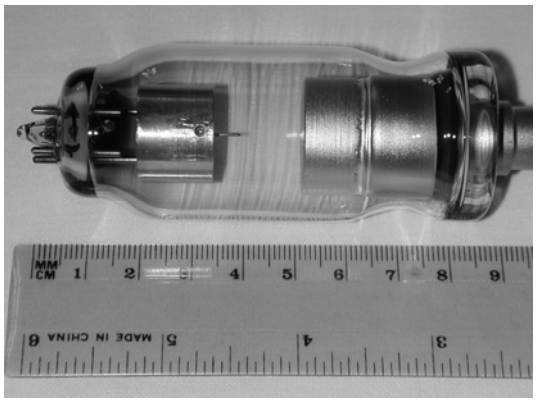

Fig. 1: Appearance of the field emission tubes made for us by Xintek.

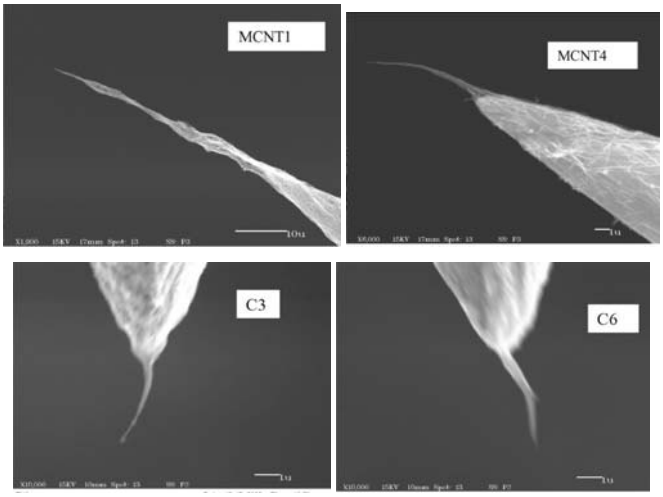

Fig. 2: SEM images of the CNT emitters in the 4 tubes.

The DC current-voltage characteristics were measured for these four tubes, as well as a field emitter tube from Leybold Didactic (Klinger, College Point, NY), which has an etched single crystal of tungsten as the emitter. All of the measurements that were made with the 5 tubes were performed at room temperature. The tungsten tip is mounted on a filament so that this tip is heated for cleaning shortly before each session of measurements. However, it is not possible to clean the CNT, which probably causes the "switch-on" effect—the supply voltage must be momentarily increased well beyond the operating point to initiate field emission with the CNT [9].

The data from the DC measurements were reduced by a Fowler-Nordheim analysis based on the following simplified form of the Fowler-Nordheim equation that gives the magnitude of the current density as a function of the applied static field for field emission from a specific material [10-12]:

$$J = A E^2 \exp(-B/E) \quad (1)$$

Here J and E are the magnitudes of the current density and the electric field intensity, $A = 1.541 \times 10^{-6}/\Phi$, and $B = 6.831 \times 10^9 \Phi^{3/2}$. The work function $\Phi = 4.5$ eV for tungsten, and for the CNT we set $\Phi = 4.9$ eV for graphene. In order to apply the Fowler-Nordheim equation to the DC current-voltage data, we also use the following equation which is valid for a given tube, where I is the field emission current and V is the potential applied between the anode and cathode:

$$I = CV^2 \exp(-D/V) \quad (2)$$

Equations (1) and (2) may be combined to obtain the following expressions for the parameters S and R, which are used to characterize the field emitters:

$$S = CD^2/AB^2 \quad (3)$$

$$R \equiv V/E = D/B \quad (4)$$

Here S is referred to as the effective emitting area, which would be the physical area of the emitter if the current density were uniform over a fixed area and zero elsewhere. The parameter R is referred to as the effective radius of curvature of the emitter, but it also includes the effects of

local intensification of the electric field caused by elongation of the emitter or the reduction of the field which may be caused by shielding due to adjacent structures.

Fowler-Nordheim plots of the DC current-voltage data were made using $\ln(I/V^2)$ as the ordinate and 1/V as the abscissa. Equation (2) requires that these plots should be straight lines, and typically the correlation $R \approx -0.998$. Linear regressions based on these Fowler-Nordheim plots typically have a standard variance $\sigma \approx 0.08$, and the probability for the null-hypothesis, that no linear relationship exists, is less than 0.0001. Values of the parameters C, D, S, and R were determined from the linear regressions.

A series ballast resistor of 100 MΩ was typically used in the measurements. However, when the series ballast resistor was increased to 2.575 GΩ with tube C-6 the data were not consistent with the Fowler-Nordheim equation ($R = -0.846$, $\sigma = 0.738$) even though the emitted current was stable at each value of the applied static potential. Fig. 3 shows the anomalous data which were obtained using the 2.575 GΩ ballast resistor. In order to explain this effect, we hypothesize that for currents greater than 500 nA, field emission with a single CNT may be intermittent, fluctuating at a high frequency. Thus, the average current, as measured by our DC microammeter, may be much greater with a large ballast resistor. This is because at those times when the current is momentarily low, the voltage drop across the ballast resistor is at a minimum so an unusually high voltage is across the tube, and this voltage causes a short-duration surge in the current.

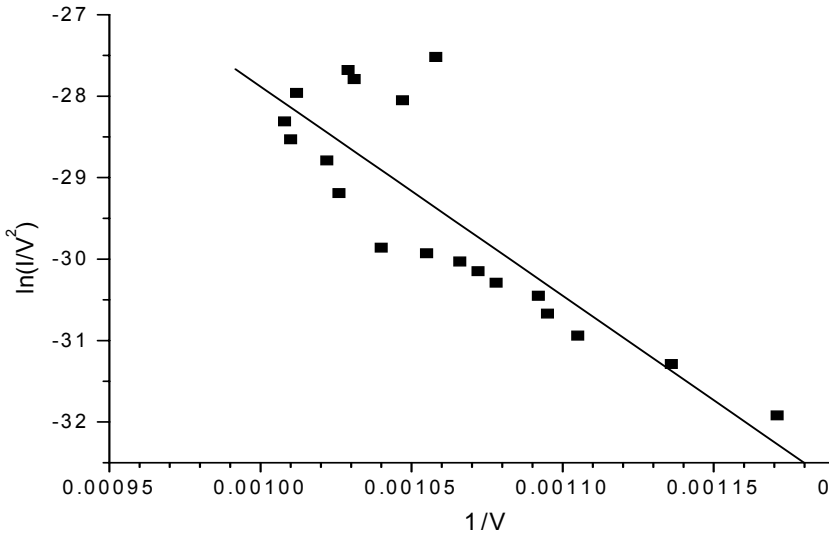

Fig. 3: Fowler-Nordheim plot for tube C-6 with a 2.575 GΩ ballast resistor.

Others have also observed instabilities in the field emission from single CNT [13-15]. However, they did not describe the bias circuits which they used so it is not possible to determine if these instabilities were exacerbated by increasing the ballast resistor. Data which are consistent with the Fowler-Nordheim equation were obtained with tube C-6 when the ballast resistor was decreased to values including 100 MΩ or 595 MΩ.

Values of the parameter R, the effective radius of curvature of the emitter, were found to vary from 77 to 110 nm for the 4 tubes with CNT emitters. This suggests that values of the local electric field at the emitting sites were as high as 14 V/nm in some of these measurements. Others studying field emission from CNT have given approximate values for the electric field by dividing the applied voltage by the distance between the anode and the emitting tip, noting that this field would be intensified by the shape of the CNT but not estimating the local electric field at the emitting sites—which would have permitted comparison with our values [4].

The Fowler-Nordheim analysis gave a value of 91 nm for the effective radius of curvature of the emitter in the Leybold tube, suggesting that the local electric field was as high as 5 V/nm in some of our measurements. Current densities as high as 10^9 and 10^{12} A/m^2 may be drawn from a tungsten emitter in steady-state and pulsed operation, respectively [12], and the corresponding values of the applied static field are 4.7 and 8.6 V/nm [3] which may be

considered as limiting field strengths for tungsten under these conditions. Thus, the value of the parameter R which we obtained for the Leybold tube appears to be reasonable.

The Fowler-Nordheim analysis also showed that the parameter S, the effective emitting area, varied from 81 to 230 nm^2 for the 4 tubes with CNT emitters. If the current density were uniform, this would correspond to circular emitting spots having radii of approximately 5 to 9 nm. Others have recently used Lorenz microscopy to directly observe the emitting sites for field emission from MWCNT, and they find one or more sites having radii of several nm [16]. Their data are in reasonable agreement with our results. The Fowler-Nordheim analysis also shows that the effective emitting area for the tungsten tip in the Leybold tube would correspond to a hemisphere with a radius of 290 nm. This result and the value of 91 nm for the effective radius of curvature of the emitter in the Leybold tube are in reasonable agreement with the radius of 100 to 200 nm which is specified by Leybold.

Measurement of Mixing at Audio Frequencies

We have made rigorous quantum simulations of laser-assisted field emission [17] which show that the radiation from 2 lasers increases the DC current (optical rectification) and also causes harmonics and mixing terms with frequencies $n_1f_1 + n_2f_2$, where f_1 and f_2 are the frequencies of the lasers and the integers n_1 and n_2 may be positive, zero, or negative. However, the high-frequency terms are not seen in measurements of the current that passes through a field emission tube because the tube itself acts as a low-pass filter [18]. We have made antennas and transmission lines on field emitters to couple microwave output power at the difference frequency $(f_1–f_2)$ [1, 19], but these techniques were not implemented in the 5 tubes for this project. Instead, we determined the spectrum of the field emission current when transformers were used to superimpose low-frequency voltages on the applied static field, with f_1 = 1.67 kHz and f_2 = 1.10 kHz. These frequencies were chosen because they are low enough that the effects of the capacitances and inductances within the tubes may be neglected [18].

To aid in understanding these phenomena, closed-form expressions for the components of the field emission current may be obtained by using time-dependent perturbation with the Fowler-Nordheim equation. This method requires the adiabatic approximation that the frequencies of the oscillatory fields are low enough that the effects of the photon energy may be neglected [1]. Thus, closed-form expressions may be determined for all of the components of the current which are found in the rigorous quantum simulations [17]. However, with laser radiation it is necessary to multiply each term by the gain that is caused by a resonance in the interaction of the tunneling electrons and the radiation field [20-23].

Consider two sinusoidal voltages superimposed on the applied static potential V_0, so that

$$V = V_0 + V_1\cos(\omega_1 t) + V_2\cos(\omega_2 t) \quad (5)$$

If V_1 andV_2 are much less than V_0 and the parameter D in Eq. (2), and the frequencies ω_1, ω_2, are low enough that the effects of the photon energy may be neglected, then a second order Taylor series expansion of Eq. (2) about the operating point (V_0, I_0), where there is only the applied static potential V_0 and the DC current I_0, gives the following expression for the total current:

$$I = I_0 + I_\Delta + I_{F1} + I_{F2} + I_{H1} + I_{H2} + I_S + I_D \quad (6)$$

The step increase of the DC current, the two fundamental terms, the two second harmonic terms, and the sum and difference terms are given by:

$$I_\Delta = I_0(D^2/4V_0^2)[(V_1/V_0)^2+(V_2/V_0)^2][1+2V_0/D+2V_0^2/D^2] \quad (7A)$$

$$I_{F1} = I_0(D/V_0)(V_1/V_0)[1+2V_0/D]\cos(\omega_1 t) \quad (7B)$$

$$I_{F2} = I_0(D/V_0)(V_2/V_0)[1+2V_0/D]\cos(\omega_2 t) \quad (7C)$$

$$I_{H1} = I_0(D^2/4V_0^2)(V_1/V_0)^2[1+2V_0/D+2V_0^2/D^2]\cos(2\omega_1 t) \quad (7D)$$

$$I_{H2} = I_0(D^2/4V_0^2)(V_2/V_0)^2[1+2V_0/D+2V_0^2/D^2]\cos(2\omega_2 t) \quad (7E)$$

$$I_S = I_0(D^2/2V_0^2)(V_1/V_0)(V_2/V_0)[1+2V_0/D+2V_0^2/D^2]\cos[(\omega_1+\omega_2)t] \quad (7F)$$

$$I_D = I_0(D^2/2V_0^2)(V_1/V_0)(V_2/V_0)[1+2V_0/D+2V_0^2/D^2]\cos[(\omega_1-\omega_2)t] \quad (7G)$$

Transformers were used to couple 2 floating battery-operated Wien bridge oscillators in series with the high-voltage anode circuit of each of the 5 field emission tubes in order to superimpose low-frequency sinusoidal signals on the applied static field. The oscillators provided the high voltages V_1=V_2=120 V which are required to cause a measurable effect on the current. The full series loop of the electrical circuit included the high-voltage power supply, a 100 MΩ ballast resistor, the secondary windings of the transformers for the oscillators, the field emission tube, a DC microammeter, and a 1 MΩ resistor to ground which was a shunt for the digital oscilloscope.

Capacitive shunts were used to eliminate the effects of the high-voltage power supply, the ballast resistor, and the DC microammeter on the currents at the 6 frequencies. Thus, the DC equivalent circuit consists of the high-voltage power supply, a resistance of 101 MΩ, the tube modeled by the two current sources I_0 and I_Δ in parallel, and the DC microammeter. The equivalent circuit at each of the 6 frequencies consists of the tube modeled by the respective current source, in series with the parallel combination of the 1 MΩ resistor and the digital oscilloscope.

The 2 oscillators were set to the frequencies f_1 = 1.67 kHz and f_2 = 1.10 kHz, and we determined the step increase in the DC current as well as the components of the current at the 6 frequencies f_1, f_2, $2f_1$, $2f_2$, $f_1 + f_2$, and $f_1 - f_2$. These frequencies correspond to 1.67, 1.10, 3.34, 2.20, 2.77 and 0.57 kHz, respectively. Each of the measured currents were compared with values calculated using the respective equivalent circuit with the expressions in Eqs. (7A-7G).

With the Leybold tube we found that the currents at the fundamental frequencies f_1 and f_2 were each within 5% of the predicted values, and the step increase in the DC current and the currents at each of the other 4 frequencies were each within 10% of the predicted values. The measured increase in the DC current, and the currents at the 6 frequencies, were each between 1 and 2 times the predicted values for tubes M-4 and C-6, and between 3 and 4 times the predicted values for tube M-1. In this series of measurements tube C-3 was too unstable to permit measuring any of the currents at the 6 frequencies. As it was noted earlier, it is not possible to clean the CNT, and this causes the values of the parameter D in Eqs. (7A-7G) to be less reproducible for the CNT than it is for the Leybold tube. We attribute the greater errors in the measurements with the CNT to this effect.

Measurement of the Change in the DC Current Caused by a Laser

While there is no means to couple microwave or THz power from any of these 5 tubes, we did measure the step increase in the DC current that is caused by focusing a single square-wave modulated laser diode (20 mW, 658 nm) on the field emission tip. The laser diode was maximally-focused to provide a measured Gaussian profile with a power flux density of approximately 10^7 W/m^2 at the tip. Equations (7A) and (7G) show that this measured current step is equal to one-half of the peak value of the mixer current that would be generated if two stabilized tunable lasers each provided the same power flux density. Thus, this low-frequency measurement may be used to estimate the mixer current which could be obtained by photomixing with these same field emitters.

The laser diode was amplitude-modulated with a square-wave envelope and the field emission current was measured with a digital oscilloscope as shown in the diagram of Fig. 4. It was noted earlier that the field emission tube itself acts as a low-pass filter. Equation (7A) shows that the increase in the field emission current, I_Δ, acts as a current source, and it is easily shown that when a square-wave current source is fed to a parallel R-C circuit, the voltage across the resistor has a saw-tooth waveform with a peak-to-peak value that is given by

$$V_{pp} = R\, I_\Delta\, (1 - e^{-1/2\tau f}) / (1 + e^{-1/2\tau f}) \qquad (8)$$

where I_Δ is the peak-to-peak value of the current waveform and $\tau \equiv RC$. Equation (8) shows that $V_{pp0} \equiv V_{pp}(f = 0) = R\, I_\Delta$, and $V_{pp} = R\, I_\Delta/4\tau f = V_{pp0}/4\tau f$ for $f >> 1/\tau$.

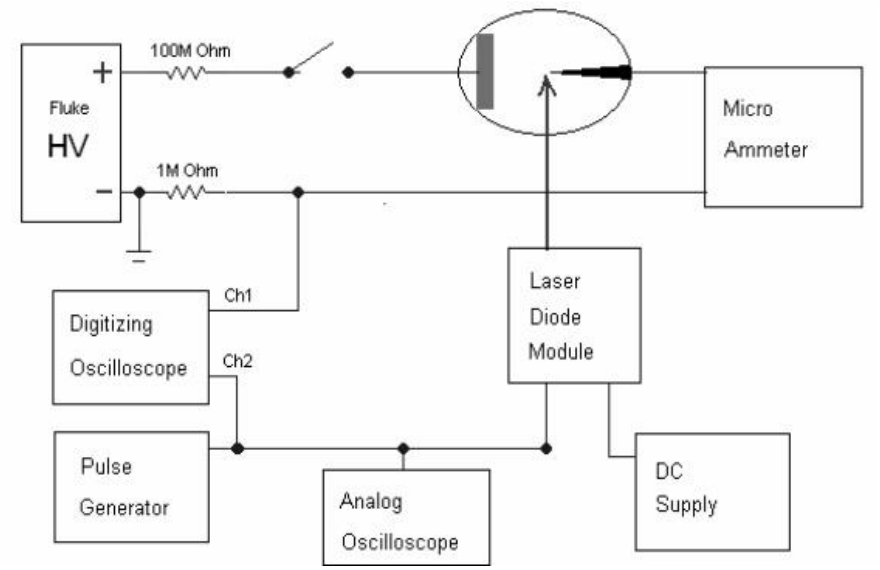

Fig. 4: Experimental configuration for measurements with a square-wave modulated laser diode.

The peak-to-peak value of the voltage across the resistor was measured as a function of the modulation frequency for each of the tubes. A DC current of 1 μA was used with each of the 4 CNT tubes, and 8 μA was used with the Leybold tube. However, tube C-6 could not be used in this test because ripples in the glass envelope interfered with focusing of the laser on the tip. Least-square regression was used to determine the values of I_Δ and τ from these data.

Table I shows the parameters that were measured with calculated characteristics of the tubes, and Fig. 5 shows the measured value of the apparent peak-to-peak amplitude of the field emission current as a function of the modulation frequency for tube M-4. This figure shows the inverse behavior which is predicted at frequencies which are much greater than $1/\tau$. From Table I, the actual value of I_Δ for tube M-4 is 83 pA, which is seen in the data that were taken for much lower modulation frequencies. Table I also shows that the mean increase in the DC current is 6.2 % for the 3 tubes with CNT, as compared with 0.20 % for the Leybold tube. This suggests that if two stabilized tunable lasers each provided the same power flux density, the peak value of the mixer current, occurring at the difference frequency (f_1–f_2), would be an average of 12 % of the DC current for the tubes with CNT, as compared with 0.40 % for the Leybold tube.

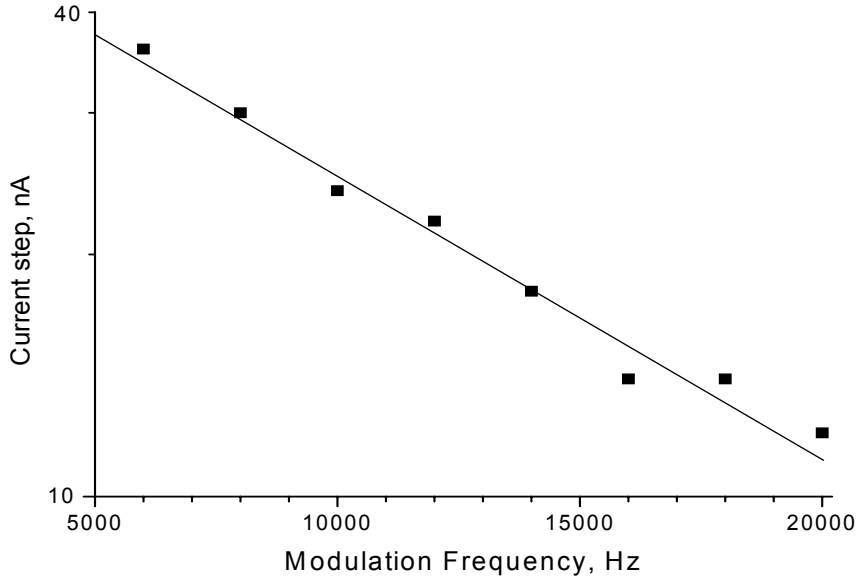

Fig. 5: Step in current caused by the laser vs. modulation frequency for tube M-4.

Table I: Measured and calculated parameters for the step-increase in the DC current caused by a laser

Tube	M-1	M-4	C-3	Leybold
I_0, the DC current, μA	1.0	1.0	1.0	8.0
DC voltage across tube, V	980	840	920	4600
R, kΩ	500	500	500	1000
T, μs	110	80	86	510
C, pF	220	160	170	510
I_Δ, pA	56	83	48	16
I_Δ / I_0, %	5.6	8.3	4.8	0.20

Discussion and Conclusions

Four field emission tubes having single CNT as the emitters were tested, and a tube having a tungsten tip was used for comparison. Fowler-Nordheim analysis of the DC current-voltage data gave reasonable values for the local fields at the emitters and the sizes of the emitter sites. Also, two audio-frequency oscillators superimposed sinusoidal signals on the applied static field, thus increasing the DC emitted current and causing components of the current at the two fundamental frequencies, the second harmonics, and the sum and difference frequencies, which are in reasonable agreement with theory. A single square-wave modulated laser diode (20 mW, 658 nm) focused on each emitter, increased the emitted current by an average of 6.2 % during each laser pulse with the CNT and 0.20 % with the tungsten tip.

We have previously made tubes in which antennas and transmission lines couple the microwave power that is generated by photomixing in laser-assisted field emission to an external load, and these tubes have used emitters of tungsten and molybdenum [1, 18]. The present measurements made with the CNT suggest that the mixer current could be 30 times greater if either SWCNT or MWCNT were used in place of the metal emitters, which would increase the microwave output power by 30 dB as a considerable improvement.

Twenty years ago there was considerable controversy regarding the mechanism by which laser radiation increases field emission current. For example, it was observed that when the laser beam is turned on the field emission current increases with a characteristic time that is similar to the calculated thermal relaxation time of the field emitter, so this effect could be thermal [24]. However, we have shown that the slow rise time for the current in such experiments is due to circuit effects, such as that which is described in relation to Eq. (8) of the present paper [25]. Recently, others have generated electron pulses with durations of under 70 fs by irradiating a field emitter with a low-power femtosecond laser [26]. They have shown that this effect is non-thermal; the operating parameters may cause either photofield emission or optical field emission to be dominant. More pertinently, others have used laser radiation to increase the field emission current from a cathode with a dense field of CNT by a factor of 18, and they have shown that this is not a thermal effect by comparing their data with the effect of elevated temperatures on the field emission from CNT [27].

Acknowledgment

This work was supported by the National Science Foundation under Grant No. DMI-0338928.

References

1. M. J. Hagmann. (2003). Appl. Phys. Lett. 83, 1.
2. M. J. Hagmann. (1998). Int. J. Quant. Chem. 70, 703.
3. M. J. Hagmann. (1999). Ultramicroscopy 79, 115.
4. A. N. Obraztsov, I. Paviovsky, A. P. Volkov, E. D. Obraztsova, A. L. Chuvilin and V. L. Kuznetsov. (2000). J. Vac. Sci. Technol. B, 18, 1059.
5. P. J. Burke. (2002). IEEE Trans. Nanotechnology, 1, 129.
6. R. Tarkiainen, M. Ahlskog, J. Penttila, L. Roschier, P. Hakonen, M. Paalanen and E. Sonin. (2001). Phys. Rev. B 64, 195412.
7. M. J. Hagmann. (1995). IEEE Trans. Nanotechnology 4, 289.
8. M. J. Hagmann and M. S. Mousa. (2006). Technical Digest, Vacuum Nanoelectronics Conference 2006 and International Field Emission Symposium (IVNC/IFES) pp. 201-202.
9. Y. Liu and S. Fan. (2005). Solid State Commun. 133, 131.
10. R.H. Fowler and L. W. Nordheim. (1928). Proc. R. Soc. Lond. A, Math. Phys. Sci. 119, 173.
11. L.W. Nordheim. (1928). Proc. R. Soc. Lond. A, Math Phys. Sci. 121, 626.
12. R. Gomer. (1993). *Field Emission and Field Ionization* (American Institute of Physics, New York).
13. J.–M. Bonard, K. A. Dean, B. F. Coll and C. Klinke. (2002). Phys. Rev. Lett. 89, 197602.
14. K. A. Dean and B. R. Chalamala. (2000). Appl. Phys. Lett. 76, 375.
15. J.-M. Bonard, J.-P. Salvetat, T. Stöckli, L. Forró and A. Châtelain. (1999). Appl. Phys. A 69, 245.
16. T. Fujieda, K. Hidaka, M. Hayashibara, T. Kamino, Y. Ose, H. Abe, T. Shimizu and H. Tokumoto. (2005). Jpn. J. Appl. Phys. 44, 1661.
17. M. J. Hagmann. (1999). Int. J. Quant. Chem. 75, 417.
18. M. J. Hagmann, M. S. Mousa, M. Brugat, E. P. Sheshin and A. S. Baturin. (2004). Surf. Interface Anal. 36, 402.
19. K. Alonso and M. J. Hagmann. (2001). J. Vac. Sci. Technol. B 19, 68.
20. M. J. Hagmann. (1995). J. Appl. Phys. 78, 25.
21. A. Mayer and J.-P. Vigneron. (2000). Phys. Rev. B. 62**,** 16138.
22. A. Mayer, N. M. Miskovsky and P. H. Cutler. (2002). Phys. Rev. B 65**,** 195416.
23. A. Mayer, N. M. Miskovsky and P. H. Cutler. (2003). J. Vac. Sci. Technol. B 21**,** 395.
24. M. J. G. Lee and E. S. Robins. (1989). J. Appl. Phys. 65, 1699.
25. M. Brugat, M. S. Mousa, E. P. Sheshin and M. J. Hagmann. (2002). Mater. Sci. Eng. A. 327, 7.
26. P. Hommelhoff, Y. Sortais, A. Anghajani-Talesh and M. A. Kasevich. (2006). Phys. Rev. Lett. 96, 077401.
27. H.-F. Cheng, Y.-S. Hsieh, Y.-C. Chen and I.-N. Lin. (2004). Diam. Relat. Mater. 13, 1004.